Analysis of a Multiple Reception Model for Processing Images From the Solid-State Imaging Camera

T.-Y. Yan
Communications Systems Research Section

This article describes a detection model to identify the presence of Galileo optical communications from an Earth-based Transmitter (GOPEX) signal by processing multiple signal receptions extracted from the camera images. The model decomposes a multi-signal reception camera image into a set of images so that the location of the pixel being illuminated is known a priori and the laser can illuminate only one pixel at each reception instance. Numerical results show that if effects on the pointing error due to atmospheric refraction can be controlled to between 20–30 μrad, the beam divergence of the GOPEX laser should be adjusted to be between 30–40 μrad when the spacecraft is 30,000,000 km away from Earth. Furthermore, increasing beyond five the number of receptions for processing will not produce a significant detection probability advantage.

I. Introduction

The trajectory of the Galileo spacecraft after the second Earth flyby in December 1992 allows Galileo optical communications from an Earth-based Transmitter (GOPEX) demonstration against a dark-Earth background [1]. Furthermore, as the spacecraft rises to an elevation as high as 55 deg, the deleterious effects of refraction associated with the laser transmissions through the atmosphere will be reduced substantially. Because of these two factors, the Earth-2 flyby has always been regarded as a prime opportunity for the GOPEX demonstration.

Against a dark-Earth background, the GOPEX laser strength received at the spacecraft will produce adequate signal to noise levels, even when the spacecraft is 30,000,000 km away. However, pointing errors will significantly degrade the signal strength at the spacecraft and subsequently reduce the probability of detecting a laser pulse by the solid-state-imaging (SSI) camera. Detection of the laser signal is of particular concern because, as the spacecraft recedes from Earth, the signal strength at the camera decreases. Different strategies for processing the images must therefore be used to ascertain whether the laser signal was detected by the camera.

The strategy for laser transmissions to Galileo will differ over the proposed 28-day course of experiments. Close to Earth, the camera shutter will remain open for only a

few tens of milliseconds to prevent lateral blooming of the camera pixels imaging the bright Earth onto those pixels containing the laser transmissions against a dark-Earth background. At the 30-Hz maximum laser-transmission rate, only one or two transmitted pulses are expected to be captured in a single camera frame. However, as the spacecraft recedes, the Earth will subtend fewer pixels in the focal plane of the SSI, and the camera shutter could be kept open for a longer period (approximately 400 msec) before lateral blooming affects the laser-illuminated pixels. Figure 1 shows a sample image of the GOPEX laser transmission.

It is expected that for a given set of input conditions, the probability of detecting the laser transmission increases with the number of received laser pulses available for processing in a given frame. Thus, at the longer ranges, where the laser signal is reduced, scanning the camera across the image of the Earth to illuminate several pixels with the laser transmission will serve not only to augment the deep-space communication demonstration, but also as a tool in processing the returned data to enhance the probability of identifying the transmitted laser signal.

This article describes a mathematical model to analyze the detection probability for the case of several laser pulses on a single frame. This analysis addresses the transmission and detection strategies for the longer ranges when the SSI camera is to be scanned across the image of the Earth. In particular, numerical examples are given for when the spacecraft is 30,000,000 km away from the Earth.

The multiple independent reception analysis presented here extends the single reception-detection model in [1]. It is the second step in the development of a comprehensive model to analyze the probability of detecting the laser transmission under actual conditions expected during the Earth-2 flyby. In the current analysis, the effects of Earth rotation and the relative velocity between the spacecraft and Earth are ignored, and it is assumed that the GOPEX laser pulse illuminates a single pixel with a known location.

II. Mathematical Model

The analysis begins with the hypothesis that when the GOPEX laser pulse is transmitted, it is called H_1, and when the laser pulse is not transmitted, it is called H_0. A total of N receptions are assumed to be available for processing. The detection processor will not determine which hypothesis is true until all N receptions are processed. Further, the receptions are assumed to be sufficiently apart so that they can be considered to be independent of one another. Let r_i be the received number of photoelectrons at the ith reception. Under the two hypotheses, then

$$H_1 \quad : \quad r_i = s_i + e_i + n_i$$

$$H_0 \quad : \quad r_i = e_i + n_i, \qquad i = 1, \ldots, N \tag{1}$$

where s_i is a Gaussian random variable representing the number of photoelectrons due to the GOPEX laser with mean μ_s and variance σ_s; e_i is a Gaussian random variable representing the number of received photoelectrons due to earthshine with mean μ_e and variance σ_e; and n is a Gaussian random variable representing other disturbances with zero mean and variance σ_n. The random variables s_i, e_i, and n_i are uncorrelated relative to one another.

Define $\Lambda(\mathbf{r})$ to be the likelihood ratio of the two hypotheses where $\mathbf{r} = (r_1, r_2, \ldots, r_N)$ is the received random vector. Then

$$\Lambda(\mathbf{r}) = \prod_{i=1}^{N} \left\{ \frac{\frac{1}{\sqrt{2\pi\sigma_1^2}} e^{-\frac{(r_i - \mu_s - \mu_e)^2}{2\sigma_1^2}}}{\frac{1}{\sqrt{2\pi\sigma_0^2}} e^{-\frac{(r_i - \mu_e)^2}{2\sigma_0^2}}} \right\} \tag{2}$$

where $\sigma_1^2 = \sigma_s^2 + \sigma_e^2 + \sigma_n^2$ and $\sigma_0^2 = \sigma_e^2 + \sigma_n^2$.

Under the Neyman-Pearson criterion, the probability of detection can be maximized by setting the detection threshold γ to the log likelihood ratio for a given probability of false alarm. From Eq. (2), setting $\ell(\mathbf{r}) = \ln \Lambda(\mathbf{r})$, the optimal detection processor is given by

$$\ell(\mathbf{r}) = -\frac{1}{2\sigma_1^2} \sum_{i=1}^{N} (r_i - \mu_s - \mu_e)^2$$

$$+ \frac{1}{2\sigma_0^2} \sum_{i=1}^{N} (r_i - \mu_e)^2 + N \ln \left(\frac{\sigma_0}{\sigma_1} \right) \tag{3}$$

The processor will declare the existence of the GOPEX laser pulse if Eq. (3) exceeds the threshold γ. In Eq. (3), the optimal processor is the difference of two quadratic forms. Each of the summations in Eq. (3) has a noncentral χ^2 distribution. Although the probability density function of the random variable ℓ (the log likelihood ratio) can be computed numerically, the approximation provided

by using the moment-generating function is much simpler and intuitive. It is generally adequate to predict the performance of the optimal detector.

Define P_{fa} to be the probability of false alarm (i.e., the laser is transmitted when it is not) and define P_d to be the probability of detection (i.e., the laser is transmitted when it is). From [2], the probability of false alarm and the probability of detection can be approximated by

$$P_{fa} \approx e^{\xi(s)-s\dot{\xi}(s)+s^2/2\ddot{\xi}(s)} \cdot Q\left(s\sqrt{\ddot{\xi}(s)}\right) \qquad (4)$$

and

$$P_d \approx e^{\xi(s)+(1-s)\dot{\xi}(s)+(s-1)^2/2\ddot{\xi}(s)} \cdot Q\left((1-s)\sqrt{\ddot{\xi}(s)}\right) \qquad (5)$$

where $\xi(s)$, $\dot{\xi}(s)$, and $\ddot{\xi}(s)$ are given in Appendix A, and

$$Q(x) = \frac{1}{\sqrt{2\pi}} \int_x^\infty e^{-t^2/2} dt$$

The approximations in Eqs. (4) and (5) will give exact solutions for cases of equal variances, i.e., $\sigma_1 = \sigma_0$. This corresponds to the case of deterministic GOPEX laser transmission of μ_s. For example, by setting $\sigma_1 = \sigma_0$ and $N = 1$, this model reduces to the previous model reported in [1]. Since the approximation makes use of the Law of Large numbers, results presented here represent a tight approximation to the exact solutions for $N \geq 3$. In general, for any given probability of false alarm, a corresponding s_f can be computed by using Eq. (A-8). Substituting the resulting s_f in Eq. (A-6) gives the threshold γ. The resulting detection probability is then given by Eq. (5), which uses the same s_f.

III. Numerical Results

This section presents results of the multiple reception-detection analysis. In these calculations, a laser output energy of 0.25J at the 0.532-μm wavelength is assumed. Since the GOPEX demonstration will be conducted against a dark-Earth background, a nominal photoelectron count of 600 photon background noise is assumed when the camera shutter remains open for half a second. This count is approximately 10 percent of the background earthshine used for the Earth-1 analysis.

Figures 2 and 3 show some of the computation results. Without loss of generality, the probability of false alarm is taken to be no more than 1×10^{-6}. The noise variance of the GOPEX laser is extracted from [2]. Figure 2 plots the detection probability as a function of the beam divergence of the GOPEX laser pulse when the spacecraft is 30,000,000 km away from Earth. The curves are parametrized by the number of receptions available for processing. The pointing error is assumed to be 25 μrad for the computation. It can be seen that the maximum probability of detection increases with the number of processed receptions. However, processing more than four receptions will result in only minor improvements of the detection probability. In all four cases, the maximum probability of detection occurs between 25–40 μrad laser-beam divergence.

Figure 3 shows the probability of detection when the spacecraft is again 30,000,000 km away from Earth, with three processing receptions. The plots are parametrized by pointing errors of 20, 25, and 30 μrad. When the beam divergence is small, as compared with the pointing error, the probability of detecting the presence of the GOPEX laser pulse degenerates to the probability of searching for the GOPEX laser pulse within the space spanned by the pointing error. Consequently, the detection probability decreases as the beam divergence is reduced. On the other hand, since the intensity of the GOPEX laser pulse decreases with increasing beam divergence, the detection probability will decrease as the beam diverges. It can be seen that for all three cases, the maximum detection probability is achieved when the beam divergence is between 30–40 μrad.

These figures indicate that if the pointing error of the GOPEX laser pulse is confined to between 20–30 μrad, the beam divergence should be maintained between 30–40 μrad to maximize the detection probability when the spacecraft is 30,000,000 km from Earth. Furthermore, the detection probability can be enhanced by processing multiple receptions within the range of interest.

IV. Summary

This article describes a detection model to identify GOPEX laser transmissions by processing multiple receptions extracted from the camera image. The approach presented here is valid for $N > 3$, even if the distributions of s_i, e_i, and n_i are non-Gaussian. Numerical results show that if effects of the pointing error due to atmospheric refraction can be controlled between 20–30 μrad, the beam divergence of the GOPEX laser should be adjusted to be-

tween 30–40 μrad when the spacecraft is 30,000,000 km from Earth. Increasing the number of receptions for processing beyond four will have diminishing returns.

There are several assumptions made to reach these conclusions. First, the model assumes a priori that the location of the pixel being illuminated is known and that the laser illuminates only one pixel at each reception instance. Effects of any disturbance due to Earth rotation and the jitter of the spacecraft dynamics are not considered. Further effort will be required to include these effects and will be reported later.

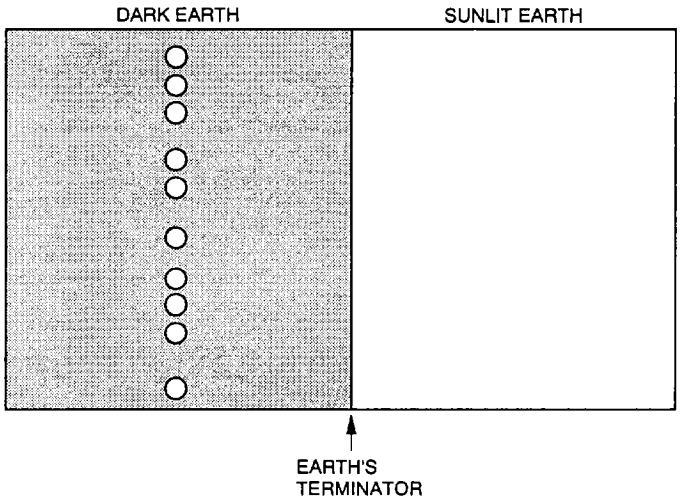

Fig. 1. A sample of GOPEX laser transmission.

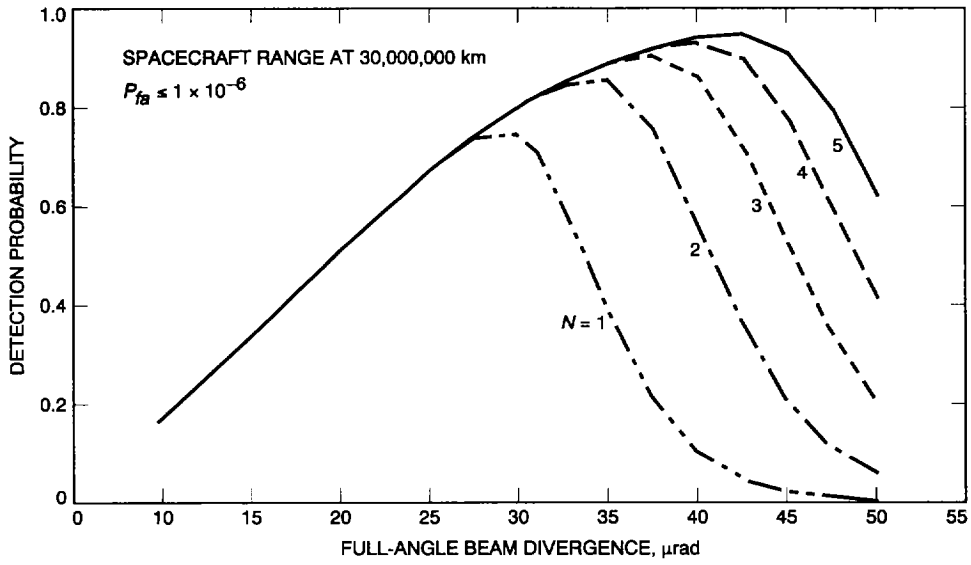

Fig. 2. Effect of increasing number of receptions on the detection probability.

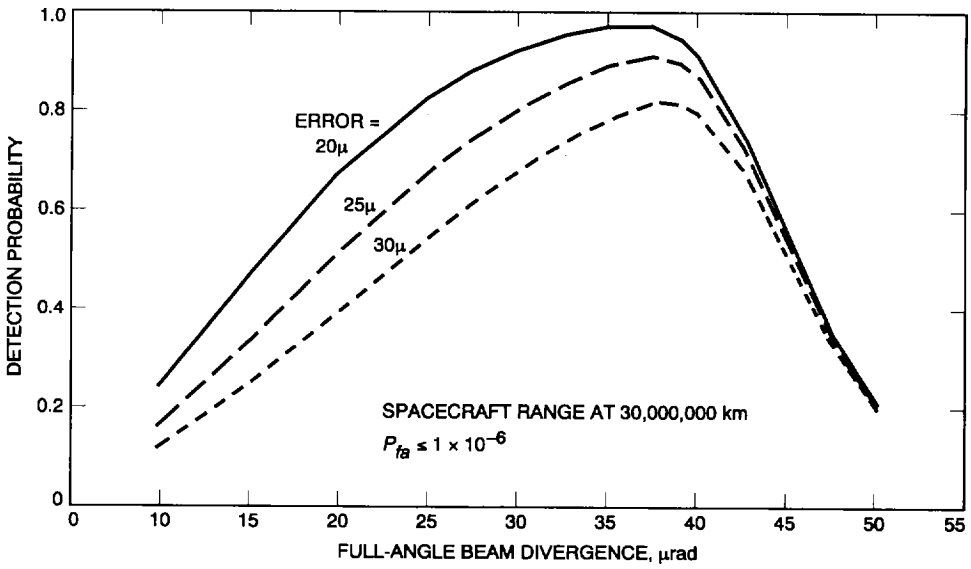

Fig. 3. Degradation of the detection probability due to laser pointing errors.

Appendix A
The Approximation of P_{fa} and P_d

The probability density functions of the received vector $\mathbf{r}$ under the two hypotheses are given respectively by

$$p(\mathbf{r}/H_1) = \prod_{i=1}^{N} \frac{1}{\sqrt{2\pi\sigma_1^2}} e^{-(r_i-\mu_s-\mu_e)^2/2\sigma_1^2} \tag{A-1}$$

and

$$p(\mathbf{r}/H_0) = \prod_{i=1}^{N} \frac{1}{\sqrt{2\pi\sigma_0^2}} e^{-(r_i-\mu_e)^2/2\sigma_0^2} \tag{A-2}$$

where $\sigma_1^2 = \sigma_s^2 + \sigma_e^2 + \sigma_n^2$ and $\sigma_0^2 = \sigma_e^2 + \sigma_n^2$.

Let

$$e^{\xi(s)} = \mathrm{E}\left[e^{s\ell(\mathbf{r})}/H_0\right] \tag{A-3}$$

be the moment-generating function of the log likelihood ratio $\ell(\mathbf{r})$ under H_0. Then, substituting Eqs. (A-1) and (A-2) in Eq. (A-3) gives

$$\xi(s) = N \ln \left\{ \int_{-\infty}^{\infty} \left[\frac{1}{\sqrt{2\pi\sigma_1^2}} e^{-(r_i-\mu_s-\mu_e)^2/2\sigma_1^2} \right]^s \times \left[\frac{1}{\sqrt{2\pi\sigma_0^2}} e^{-(r_i-\mu_e)^2/2\sigma_0^2} \right]^{1-s} dr_i \right\} \tag{A-4}$$

After some algebraic manipulations, the integral is given by

$$\xi(s) = \frac{N}{2} \left\{ \ln \left(\frac{(\sigma_1^2)^{1-s}(\sigma_0^2)^s}{s\sigma_0^2 + (1-s)\sigma_1^2} \right) + \frac{s(s-1)\mu_s^2}{s\sigma_0^2 + (1-s)\sigma_1^2} \right\} \tag{A-5}$$

Differentiating Eq. (A-5) with respect to s, one has

$$\dot{\xi}(s) = \frac{N}{2} \left\{ \ln\left(\frac{\sigma_0^2}{\sigma_1^2}\right) - \frac{\sigma_0^2 - \sigma_1^2}{s\sigma_0^2 + (1-s)\sigma_1^2} + \mu_s^2 \frac{s^2\sigma_0^2 - (s-1)^2\sigma_1^2}{[s\sigma_0^2 + (1-s)\sigma_1^2]^2} \right\} \tag{A-6}$$

The second derivative of $\xi(s)$ is given by

$$\ddot{\xi}(s) = \frac{N}{2} \left\{ \left(\frac{\sigma_0^2 - \sigma_1^2}{s\sigma_0^2 + (1-s)\sigma_1^2} \right)^2 + 2\mu_s^2 \frac{\sigma_0^2\sigma_1^2}{[s\sigma_0^2 + (1-s)\sigma_1^2]^3} \right\} \tag{A-7}$$

From [3], the probability of false alarm is

$$P_{fa} \approx e^{\xi(s) - s\dot{\xi}(s) + (s^2/2)\ddot{\xi}(s)} \cdot Q\left(s\sqrt{\ddot{\xi}(s)}\right) \tag{A-8}$$

and the probability of detection is given by

$$P_d \approx e^{\xi(s) + (1-s)\dot{\xi}(s) + [(s-1)^2/2]\ddot{\xi}(s)} \cdot Q\left((1-s)\sqrt{\ddot{\xi}(s)}\right) \tag{A-9}$$

The corresponding threshold can be determined as

$$\gamma = \dot{\xi}(s)$$

The function $Q(x)$ is given by

$$Q(x) = \frac{1}{\sqrt{2\pi}} \int_x^{\infty} e^{-t^2/2} dt$$

It should be noted that $\ddot{\xi}(s)$ must be positive in both Eqs. (A-8) and (A-9) for all values of s. The first term on the right-hand side of Eq. (A-7) is always positive. A sufficient condition for $\ddot{\xi}(s)$ to be positive is that the denominator of the second term remains positive for all values of s. Hence, the variable s is restricted by the following inequality,

$$0 \le s \le \frac{\sigma_1^2}{\sigma_1^2 - \sigma_0^2}$$

References

[1] K. E. Wilson, J. R. Lesh, T.-Y. Yan, J. Schwartz, M. D. Rayman, and S. Wee, "GOPEX: A Deep Space Optical Communications Demonstration With the Galileo Spacecraft," *TDA Progress Report 42-103*, vol. July–September 1990, pp. 262–277, November 15, 1990.

[2] K. Klaasen, M. Clary, and J. Janesick, "Charge-Coupled Device Television Camera for NASA's Galileo Mission to Jupiter," *Optical Engineering*, vol. 23, no. 3, pp. 334–342, May/June 1984.

[3] H. Van Trees, *Detection, Estimation, and Modulation Theory*, New York: John Wiley & Sons, 1968.